Chapter VIII

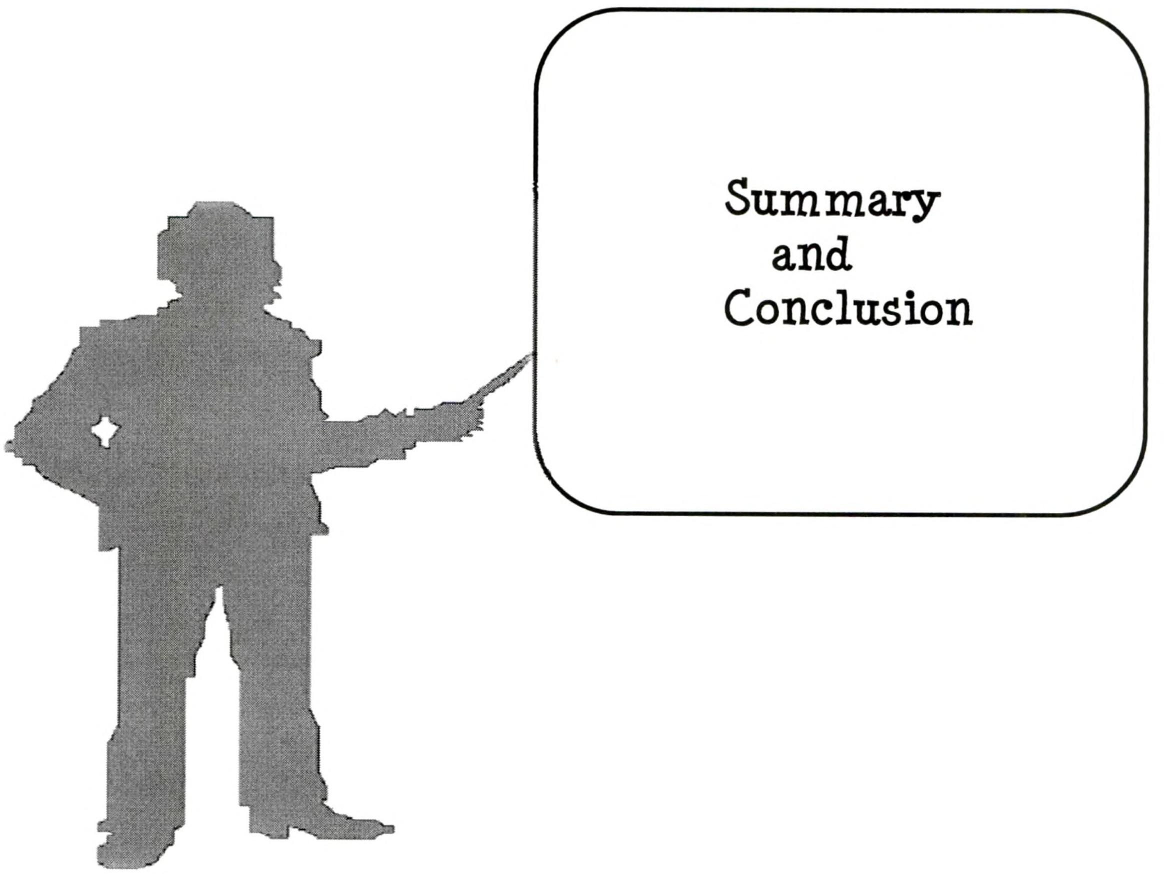

CANCER is one of the most dreaded diseases in the world. Among all types of cancers, breast cancer is most common cancer affecting females. Mainly breast cancers are treated by surgery to remove the tumor. Sometimes chemotherapy or hormonal therapy may be given to shrink a cancer before surgery. After surgery, radiotherapy may be given to eradicate cancer cells that may have left in the affected area. After surgical removal of tumors, there is always a risk of recurrence because the microscopic cancer cells may have spread to distant sites in the body which may again grow into tumor. In order to decrease the risk of recurrence, many breast cancer patients are offered chemotherapy. The standard chemotherapeutic agents that are used in treatment of breast cancer are doxorubicin, methotrexate, fluorouracil, docetaxel and paclitaxel.

Breast cancer chemotherapeutics have little selectivity for cancer cells to their higher proliferation rates. This can lead to increased toxicity against normal tissues that also show enhanced proliferative rates, such as the bone marrow, hair follicles, etc. Effective tumor chemotherapy requires targeting the anticancer drug to its molecular sites of action. Random, non-targeted distribution of the drug within the living system reduces therapeutic efficacy and at the same time, increases the risks of undesirable side effects and toxicity. The success of novel strategies for cancer therapy strongly relies on the development of formulations capable of improving the therapeutic index of biologically active molecules, mainly by increasing their concentration at the desired targeted sites while avoiding normal tissues. One strategy is to couple the therapeutics to antibodies or other ligands that recognize tumor-associated antigens. This increases the exposure of the malignant cells, and reduces the exposure of normal cells, to the ligand-targeted therapeutics. Reticuloendothelial system (RES) usually acts to fast-remove the foreign particles including novel anticancer formulations from the blood circulation, which prevents them from encashing the benefits of the leaky tumor vasculature. A breakthrough in countering this fast removal was achieved when it was found that nano sized particles, and more so a combination of small size and hydrophilic surface, delay RES uptake. A very good example of this approach is the doxorubicin loaded liposomal formulation (Doxil) which is currently in market for treatment of various cancers and more specifically in breast cancer chemotherapy.

After success of Doxil, increased attention has been paid to develop vesicular systems based on block copolymers, named polymersomes, as competent drug carrier in recent years, with some remarkable, attractive and feasible characteristics. Indeed, polymersome is one of the supramolecular self assembled structures of block copolymer in aqueous and non-aqueous media and has proved to be an emerging novel carrier for drug delivery and gene therapy. Chapter I introduces basics of block copolymer and their use in formation of nanocarriers such as polymer vesicles (Polymersomes) or polymeric micelles.

Chapter II describes synthesis of polypeptide-*block*-polysaccharide copolymers namely, poly(benzyl L-glutamate)-*block*-hyaluronan. Molecular characterizations of HYA polymer were performed by static light scattering (SLS) and SEC in acetate buffer (pH=5.6). SLS provided a weight-average molecular weight (Mw) of 5100 g/mol, polydispersity index given by SEC analysis, PDI = 1.4, and the number-average molecular weight has been derived, Mn = 3670 g/mol. This value is in good agreement with the one deduced from NMR analysis (Mn = 3790 g/mol) and corresponds to a degree of polymerization DP = 10. NMR spectroscopy of HYA confirmed the presence of a reducing end. Alkyne end-functionalized hyaluronan (HYACCH) was achieved by conventional reductive amination in 100 wt % yield and characterized by SEC, ^{1}H-NMR and IR spectroscopy. We identified all characteristic peaks of sodium hyaluronan except at δ = 5.2 ppm and δ = 5.5 ppm that are characteristic peaks of α, β anomeric protons. Therefore, the disappearance of anomeric proton peaks confirmed the functionalization of hyaluronan. In addition, IR spectra and ^{1}H-NMR shows no difference between HYACCH before and after acid treatment.

The α-azido-PBLG was obtained by ring opening polymerization (ROP) of Bz-L-GluNCA using 1-azido-3-aminopropane as initiator. This compound was fully characterized by DSC, SEC, FTIR and ^{1}H-NMR spectroscopy. FTIR analysis confirms the formation of α-azido-PBLG. In addition the band at 2097cm^{-1} confirms the functionalization of PBLG by an azide group. The molar mass was accurately determined from ^{1}H-NMR spectroscopy. A number-average degree of polymerization ($\overline{DP_n}$) of 23 was derived from NMR analysis. We also determined the polydispersity index = 1.1 by

SEC. In DSC analysis of PBLG-N_3, heating and cooling DSC traces reveal a glass temperature at 15.12°C.

Huisgen's 1, 3-dipolar cycloaddition (click reaction) was performed between the α-azide end-functionalized PBLG and α-alkyne-HYA acid (HYACCH acid). The structure of the block copolymer was determined by ^{1}H-NMR and IR analysis and 65% yield was obtained. The peak of the triazole ring was found at 7.6 ppm which indicates the coupling between both blocks by click reaction. This is also supported by data obtained by IR analysis that shows the full disappearance of azide peak at 2090 cm^{-1}. Based on the static light scattering, SEC, and ^{1}H-NMR analysis of each block and PBLG-*b*-HYA copolymer, we are able to provide the right composition of the block copolymer, namely $PBLG_{23}$-*b*-HYA_{10}.

Solution behavior of block copolymer $PBLG_{23}$-*b*-HYA_{10} is described in Chapter III. We investigated the self assembly behavior of block copolymer in tris buffer (pH 7.4) by the well-known process such as direct dissolution and nanoprecipitation method. In direct dissolution at room temperature a broad relaxation time distribution was observed that could be due to the aggregation of copolymer in Tris buffer. At 40°C a sharp peak of the size distribution was observed with a polydispersity index of 0.16 obtained from cumulant analysis. The hydrodynamic radius R_H was calculated to be 190 nm from the slope of the relaxation frequency dependency to the square scattering vector.

Nanoprecipitation method was performed at 55°C and DLS plot showed one main narrow relaxation time distribution before and after dialysis. Polydispersity indexes are 0.04 and 0.08 before and after dialysis, hydrodynamic radii being 248nm and 209nm respectively. Static light scattering measurements were also used to asses R_g/R_H. Considering the light scattering results, $PBLG_{23}$-*b*-HYA_{10} block copolymer would afford vesicular morphology in tris buffer ($Rg/R_H \sim 1$).

Vesicle morphology was attested by SANS experiments. In addition, from the slope of the representation $\ln(q^2I(q))$ versus q in the asymptotic Kratky-Porod approximation, we could estimate the thickness of the vesicle membrane $\delta \sim 9$nm. We also calculated vesicle membrane thickness theoretically ~ 9.3nm. The calculated value is in good agreement with the experimentally determined δ value from SANS.

Finally we concluded, that block copolymer ($PBLG_{23}$-*b*-HYA_{10}) formed polymersomes around 200nm in hydrodynamic radius (R_H) by their intrinsic self assembly property in tris buffer (pH 7.4) through nanoprecipitation method. A radius around 120nm has been obtained after sonication of preformed polymersomes prepared by nanoprecipitation. Polymersomes were stable at pH 9 to pH 3 in respect of their particle size and surface potential. This is in good agreement with the known pka value for hyaluronan (pKa =3). In addition, polymersomes were stable for more than 90 days at RT and at 4°C. Stability was further enhanced by lyophilization and freeze dried vesicles were easily reconstituted with tris buffer through vortexing for few minutes.

TEM and FF-TEM images show typical images of polymersomes. AFM image of polymersomes prepared by nanoprecipitation shows the soft hydrophilic hyaluronan shell, spreading around the polymersomes and strongly adsorbing onto the hydrophilic mica surface.

Doxorubicin (DOX) loading and characterization is described in Chapter IV. DOX loading was performed at different feed weight ratios (drug/copolymer) by a so called nanoprecipitation method. The maximum DOX loading in polymersomes that has been achieved was 12±1 wt% (i.e. 120µg of drug/mg of vesicles) with encapsulation efficiency of about 40% at weight ratio 0.3/1.0 (drug/copolymer). A hydrodynamic radius R_H of 220nm was measured with one main narrow relaxation time distribution and a low polydispersity value from cumulant analysis.

Morphology and characteristic sizes of polymersomes remained unaffected after loading. It is worthwhile to note that the morphology and the size of the vesicles remained constant after loading as illustrated by TEM, FF-TEM and AFM analysis. The AFM image is particularly interesting, compared to the one before loading, as it shows a dense core, due to the presence of DOX into the vesicle reservoir. DOX encapsulation in polymersomes did not affect their colloidal stability since the hydrodynamic radius of polymersomes remains unchanged with and without DOX at the pH range from 3 to 9.

Free DOX was completely released in 8h at pH 7.4 whereas $PBLG_{23}$-*b*-HYA_{10} based polymersomes modify the *in vitro* release pattern of DOX after encapsulation at pH 5.5 or 7.4. Time for 50% DOX release was around 24h at both pH, and remaining DOX was

released up to 10 days. Higuchi representation showed two linear domains in the release curve. This representation confirmed a two step release profile with two kinetic constants.

Stability of PolyDOX formulations was investigated at both RT and at 4^0C. A significant difference in loading content was observed at storage conditions RT and 4^0C. Above than 90% DOX was recovered from each PolyDOX formulation after being stored at 40^0C for 120 days whereas less than 90% DOX was obtained in each PolyDOX formulation after 15 day's storage at RT in open area. The stability of PolyDOX formulations was enhanced by lyophilization process. There was no significant difference in loading content before and after storage of lyophilized formulation at 4^0C for more than six months.

Preliminary study of cell line work was performed on C6 glioma cells for determination of *in vitro* efficacy of PolyDOX. Microscopic observations of treated cells showed distinct morphological changes indicating unhealthy cells, whereas the control cells appeared normal. Phase contrast images showed clearly different interactions of C6 cells with free DOX and PolyDOX at 3 and 24h. Free DOX treated cells appeared compact with almost same morphology as control at 3h because of diffusion mediated internalization in C6 cells and also it could be the lag phase for DOX killing on C6 cells whereas at 24h with DOX, round cells that could be dead cells with cluster of cells appeared. However, PolyDOX treated cells appeared to be clustered with cellular extensions and external buds were observed as compared to control cells, it could be due to receptor mediated endocytosis uptake.

The cytotoxicity of PolyDOX was evaluated in C6 glioma tumor cell lines by MTT assay. Control $PBLG_{23}$-*b*-HYA_{10} polymersomes without drug did not show a cytotoxic effect in the concentration range 0.1 – 700μg/mL. IC_{50} values of free DOX and PolyDOX was calculated from dose response curve. At 48h, free DOX produces IC_{50} = 1μM whereas PolyDOX have IC_{50} = 7.63μM. This difference could be explained by different internalization mechanism. Cytotoxicity measurement at 48h, performed at 5 μM concentration, showed that cells incubated with free DOX are strongly affected (80% death), while cells incubated with PolyDOX are unaffected.

Cell uptake studies were performed with free DOX and DOX-loaded vesicles. After 24h incubation with free DOX (5μM), cells changed their morphology, being retracted and ovoids, and losing their adhesion properties. These observations are typical for cells engaged in death processes, probably by apoptosis, as known with DOX. However, for similar incubation conditions with PolyDOX, most of the cells still spread and stick on the culture support. Furthermore, DOX fluorescence allows for visualisation of the drug distribution in the still living cells, either by microscopy or cytometry. After 24h incubation, fluorescence was observed for free DOX, in the cytoplasm and mostly in the nucleus of the round cells. Under the same conditions, the PolyDOX fluorescence appeared more diffuse in the cytoplasm and particularly concentrated as dots in endosomal like vesicles. This noticeable difference at intracellular level or in sub-cellular distribution of DOX suggests that PolyDOX were taken up by cells mainly via an endocytic pathway. The cytometry analysis, performed only on living cells, showed a similar level of the cell fluorescence, independently of its intracellular location as seen by microscopy. However, the large profile of fluorescence after 6h incubation of free DOX is in contrast with the thinner and higher level of fluorescence measured for PolyDOX. This difference could be relevant of a diffuse intracellular repartition of DOX, being both located in the cytoplasm and the nucleus for free DOX incubation (as observed by microscopy), opposed to a more localized concentration of PolyDOX in the cellular vesicle compartments. For 24h time point, the cytometry profile of free DOX incubated cells is in agreement with a nuclear accumulation. Moreover, the concerned cell number decreased faster for cells in the free DOX conditions, than for ones incubated with PolyDOX. As a result, the time evolution of the global fluorescence per condition showed a lag of 24h in its decrease, being the consequence of the PolyDOX compartmentalization. Indeed, this delay is representative of time involved for the shift of the DOX from the PolyDOX, and then from endosomal like vesicles to the cytoplasm, before its accumulation inside the nucleus when interacting with the DNA and produced cytotoxicity. Finally, the cellular vesicle accumulation of PolyDOX strongly suggests an endocytosis pathway, probably receptor mediated.

Chapter V describes complete cell line work on malignant cell lines U87 (human glioma) and MCF-7 (human breast cancer cells). Both cell lines used for comparative

study of DOX and PolyDOX are CD44 expressing therefore we determined relative CD44 expression to each other in both the cell lines and we observed that both cells express significant ($P<0.05$) CD44 receptor compared to unstained of their respective cells.

DOX and PolyDOX internalization in the MCF-7 and U87 cells was studied using fluorescence microscopy. Intracellular distribution of the PolyDOX is quite different from that of DOX solution. After 3h of incubation with the DOX solution in MCF-7, strong fluorescence of DOX was observed in cell nuclei in addition to the very weak fluorescence in cytoplasm, suggesting rapid intercalation of intracellular DOX to the chromosomal DNA after passive diffusion into the cells. On the other hand, PolyDOX fluorescence exhibited speckled red dots throughout the cytoplasm as well as very less in nuclei even after 48h, indicating that PolyDOX were initially trapped within endosomal compartments after cellular uptake. These data not only demonstrate that PolyDOX is an efficient vehicle to transport DOX into the cytoplasm, but also suggest that the internalization mechanism of polymersomes is different from that of free DOX. The noticeable difference in sub-cellular distribution of DOX, suggested that PolyDOX were taken up by cells mainly via an endocytic pathway and were then localized in acidic endocytic compartments (i.e. endosomes and later lysosomes).

Furthermore, the presence of p-glycoprotein pump (Pgp) in U87 cells expelled DOX from cells. Indeed, a decrease of DOX fluorescence was observed in nuclei and cytoplasm of U87 cells after 48h incubation time, whereas remarkable increase in the PolyDOX fluorescence from the cytoplasm was observed as in the case of MCF-7 cells.

Flow cytometry was used for quantitative determination of DOX uptake in cells. The results show that the DOX were successfully transported into cells by being loaded in polymersomes. The cellular uptake of DOX was significantly ($P<0.01$) higher in the samples incubated with PolyDOX than in those treated with free DOX in both MCF-7 and U87 cells, and was concentration dependent. Interestingly, compared with control of their respective cells, PolyDOX was intracellularly significantly ($P<0.001$) more accumulated in MCF-7 than U87 cells. This notable difference suggests the higher intracellular DOX concentration in PolyDOX incubated cells, can be the result of a

higher CD44 expression level in MCF-7 cells. Thus, the enhanced uptake of PolyDOX can be attributed to their facilitated CD44 receptor mediated endocytotic transport, relative to a more passive and less efficient endocytosis pathway in the case of U87 cell lines.

Presence of free HYA in the incubating media reduced DOX fluorescence intensity in PolyDOX incubated cells but almost no effect ($P>0.05$) in free DOX uptake in both cells was observed. These results demonstrate the role of HYA receptor-mediated endocytosis in efficient intracellular delivery of hyaluronan based polymersomes.

It was revealed that the non-loaded copolymer vesicles had nearly no influence to the viability of both cells in the concentration range from 150 to 650 μg/mL. We investigated the concentration effect of DOX on the viability of both cells. Two approaches were used, so called immediate effect (continuous exposure effect) and delay effect, referring respectively to the DOX effect that was measured immediately after end of treatment, and measured after an additional growth period after DOX removal from the medium. In both cases, cytotoxicity was concentration and exposure time dependent and cytotoxicity increases with increasing DOX concentration and exposure time for both free DOX and PolyDOX incubation.

DOX and PolyDOX did not show cytotoxicity at 3h in immediate effect experiment in both cells it could be the lag phase of DOX and PolyDOX, but produced cytotoxicity at 3h in delay effect experiment except in U87cells where DOX expelled from cells due to presence of Pgp pumps. DOX was potent (IC_{50} = 4.52μM) at 24h than PolyDOX (IC_{50} = 9.13μM) but less potent after 48h with continuous exposure (immediate effect) in MCF-7 cells, might be because DOX was in free form and accumulate rapidly in nucleus whereas PolyDOX releases DOX from cytosolic compartments in controlled manner and continuously produced more cytotoxicity at 48, 72 and 96h. PolyDOX was revealed more potent at each exposure time points (3-96h) than free DOX in delay effect experiment in both cells.

The IC_{50} values of PolyDOX were less in each time points either its immediate effect experiment or delay effect experiment in MCF-7 cells than U87 cells. In addition, IC_{50} values revealed that PolyDOX was cytotoxic in both CD44 receptor expressing cells

(MCF-7 and U87) and more precisely much potent in MCF-7 than U87 by factor of 1.5 at 48h in immediate effect experiment and by factor of 3.2 at 24h in delay effect experiment. It could be due to difference in CD44 receptor level in both cells therefore PolyDOX enhanced high accumulation of DOX intracellularly via highly expressed CD44 mediated endocytosis in MCF-7.

Surprisingly, PolyDOX increased significantly ($P<0.001$) ROS level in both cell lines compared to free DOX at 24h, and DOX mediated ROS level was also significant ($P<0.05$) compared to control cells (without treatment) because DOX is well known for induction of ROS generation. Therefore, predictable death mechanism for PolyDOX could be that PolyDOX was more accumulated intracellularly in endosomal, lysosomal and mitochondrial compartments after receptor mediated endocytosis, where it released DOX in a controlled manner and generated ROS level which is directly related to the cellular death.

Free DOX and PolyDOX suppressed significantly tumor growth as compared to PBS control group. However, PolyDOX showed higher tumor suppression than the free DOX ($P<0.05$). The high antitumor activity of the PolyDOX can be attributed to a higher accumulation in cancer cells, a controlled release feature and a decreased influence of MDR effect. Almost negligible tumor burden was achieved after treatment with PolyDOX compared to control and free DOX treatment. Kaplan-Meier survival curve shown after IV injection of PolyDOX showed enhanced survival time for tumor bearing rats and no mortality was observed after 60 days post treatment.

In addition, DOX mediated induction in serum enzymes (LDH and CPK) was low after encapsulation in polymersomes compared to free DOX. Therefore, reduced level of LDH and CPK by PolyDOX formulation indicates reduced cardiotoxicity of DOX after encapsulation in polymersomes, in agreement with a significant reduction of side-effects and mortality.

In Chapter VI, we had demonstrated *in vivo* efficacy of PolyDOX. We used Ehrlich Ascites Tumor model for *in vivo* studies which is a transplantable tumor that arises from a mouse mammary adenocarcinoma and it grows in both ascitic and solid forms. ^{99m}Tc radionuclide was used for determination of *in vivo* efficacy of PolyDOX.

All compounds were efficiently labelled with ^{99m}Tc by direct labeling method and produced stable radio labeled complex at *in vitro* and *in vivo* conditions. Particle sizes of PolyDOX and Blank-POLY did not change after incubation with human serum for 48h at 37^0C.

All the ^{99m}Tc-labeled compounds were rapidly cleared from the blood circulation. However, there was significant difference ($P<0.01$) in plasma profile between the injected ^{99m}Tc-labeled compounds. PolyDOX concentration was significantly higher ($P<0.001$) in bloodstream than that of free DOX at each sampling time points whereas no significant difference ($P>0.05$) was found between PolyDOX and Blank-POLY.

The PolyDOX significantly increased the half-life ($T_{1/2}$; 19.48h), mean residence time (MRT; 24.72h) and area under the curve (AUC; 59.61% h/mL) of DOX in circulation, as compared with free DOX ($T_{1/2}$; 5.54h, MRT; 6.99 h, AUC; 24.26% h/ml,). These results indicate that PolyDOX can circulate for a longer time in the blood circulation system than free DOX.

Flow cytometry result shows significantly expressed CD44 receptor level in EAT cells. Therefore, EAT model was good choice to determine the efficacy of PolyDOX.

Tissue uptake of PolyDOX was significant ($P<0.01$) in each organs than free DOX. Results showed the liver > spleen > lungs to be the organs of preferential accumulation of ^{99m}Tc-PolyDOX. PolyDOX uptake was significantly high ($P<0.01$) in liver and low ($P<0.01$) in heart compared to free DOX.

PolyDOX reduced significantly ($P<0.05$) the uptake ratio between liver/blood than DOX which indicate PolyDOX clearance was delayed compared to free DOX after IV injection of PolyDOX. After 1h, tumor uptake of free DOX was significant ($P<0.01$) but later on PolyDOX uptake was increased significantly ($P<0.001$) compared to free DOX. In addition, we also determined ratio of uptake of free DOX and PolyDOX between tumor and muscle (opposite side than tumor). In addition, we also determined ratio of uptake of free DOX and PolyDOX between tumor and muscle (opposite side than tumor) (Figure 6.7B). Interestingly, PolyDOX showed high ratio of uptake between tumor and muscles and was significantly higher than free DOX ($P <0.001$).

Notably, PolyDOX concentration was found lower and significant ($P<0.001$) in the heart at all time points. Therefore using PolyDOX formulation could reduce cardiac toxicity of free DOX because of low uptake.

Animals receiving a total dose of 15 mg/kg free DOX administered by 3 injections (3×5mg/kg/day) died within 17days from first injection. This can be correlated to LD_{50} (lethal dose killing 50% of the test animals) of DOX, is generally 12.7-13.2 mg/kg. However, other treated groups showed extended survival for more than a month.

No considerable difference in blood parameters was observed after treatment with PolyDOX (5, 15, 20 mg/kg) and with Blank-POLY (20mg/kg) in healthy mice. In contrast, free DOX received animals showed considerable differences from the control group for WBC, Platelets counts and lymphocytes.

It is noteworthy that the levels of CPK (creatine phosphokinase), LDH, (lactate dehydrogenase), aminotransferases (ALT and AST) and creatinine and BUN were normal in groups treated with PolyDOX (5, 15 20 mg/kg) and with Blank-POLY (20mg/kg), indicating that the heart, liver and renal functions were normal. However, mice treated with free DOX (5 and 15mg/kg) showed considerable difference in level of serum enzymes compared to control.

Histopathological analysis after IV administration of DOX (15mg/kg) on 7 days after last dose resulted in loss of myocardial tissue, focal necrosis of muscle fibers with eosinophilia in the cytoplasm, disarray and destruction of muscle fibers with focal hemorrhage. However, PolyDOX (20mg/kg) treated group on 21 days exhibit relatively normal myocardial cells with vascular dilatation and reasonable degeneration of some fibril cells, compared to the control. DOX (15mg/kg) treated mice showed diffuse fatty degeneration and necrotic changes in the liver. PolyDOX (20mg/kg) treated mice showed similar change, but all were milder than DOX (15mg/kg) treated mice. There were no significant abnormalities observed in the other organ tissues treated with PolyDOX.

Blank-POLY did not show hemolytic activity even at high concentration (500µg/mL). However, slight hemolysis (approximately 4%) was observed in case of PolyDOX. PolyDOX could release DOX in experimental conditions because it releases DOX ~ 30%

in 1h at 37°C *in vitro*. Therefore, the leakage of hemoglobin from the RBC could be attributed to the action of released DOX on the cell membranes.

PolyDOX suppressed the tumor growth significantly ($P<0.01$) then control. PolyDOX dominantly control tumor growth compared to free DOX ($P<0.01$). In addition PolyDOX significantly ($P<0.01$) delay doubling time of EAT tumor compared to control and DOX treated group whereas no difference ($P>0.05$) in doubling time of EAT tumor between free DOX and control group animals.

A combined effect of the passive targeting and active targeting would be the main reason for the suppression of tumor growth in case of PolyDOX. PolyDOX treated mice was able to survive for more than 2.5 months. We calculated Increase in Life Span (ILS) from the survival data and plotted. PolyDOX increases ILS 6 times more than free DOX. It is rational to expect that the higher DOX levels of the PolyDOX in the tumor would result in higher therapeutic potency. It can be attested from gamma scintigraphy images that PolyDOX was accumulated in tumor.

We demonstrated loading of docetaxel, *in vitro* and *in vivo* characterization in Chapter VII. We took the opportunity to encapsulate docetaxel (DOC) anticancer drug as hydrophobic model drug in polymersomes and determine their efficacy *in vitro* and *in vivo*.

DOC loading was determined at different feed weight ratio (drug/copolymer) by nanoprecipitation. Maximum DOC loading in polymersomes was 9.81 ± 0.66 % (i.e. ~100μg of drug/mg of polymersomes) with encapsulation efficiency of about 49%. The hydrodynamic radius of PolyDOC was determined to be $R_H = 135 \pm 10$nm by dynamic light scattering (DLS) after sonication of preformed PolyDOC.

Typical, PolyDOC morphologically was obtained by freeze fracture-TEM and AFM. Stability of PolyDOC formulations was examined at both RT and at 4^0C for one month. Above than 90% DOC was recovered after storage of PolyDOC at 4^0C. However, PolyDOC is also stable at RT except 0.2:1 batch; it shows few particles or crystals which we considered to be not a stable formulation in one month storage at RT. The stability of PolyDOC formulations was enhanced by lyophilization process. There was no significant

difference in loading content before and after storage of lyophilized formulation at 4^0C for more than six months.

Free DOC was completely released in 4h whereas sustain release behavior of DOC was observed in both pH (pH 5.5 and 7.5) after being loaded in Polymersomes. PolyDOC released more than 20% of DOC in 24h and remaining DOC was released up to 10 days. Diffusion release kinetics was found from Higuchi model representation.

The *in vitro* cytotoxicity of the free DOC, and PolyDOC was evaluated using the MCF-7 cells and U87 cells that are positive for CD44 receptor for hyaluronan with high expression (MCF-7) and low expression (U87). Cytotoxicity was dependent on exposure time and concentration of free DOC, and PolyDOC. Cell viability decreased as exposure time and concentration of compounds increased in both cells. Free DOC was significantly potent ($P<0.05$) at 24h but at 72h PolyDOC produced significant ($P<0.01$) cytotoxicity compared to free DOC in MCF-7 cells. U87 cells express p-glycoprotein pump (Pgp) therefore viability was not affected after exposure with free DOC at 24h. PolyDOC produced significant ($P<0.01$) cytotoxicity in both cells compared to free DOC at 72h. MCF-7 cells express high CD44 hyaluronan receptor level compared to U87 therefore PolyDOC was significantly more potent in MCF-7 cells than U87 cells in each time point.

All compounds were labelled with ^{99m}Tc by direct labeling method and represent more than 98% labeling efficiency together with less than 2% impurities. Radio labeled complexes were stable at *in vitro* and *in vivo* conditions.

Significant difference ($P<0.01$) in plasma profile was obtained between the injected ^{99m}Tc-PolyDOC and ^{99m}Tc-DS (Docetaxel solution). PolyDOC concentration was significantly higher ($P<0.001$) in bloodstream than that of DS (Docetaxel solution) at each sampling time.

The PolyDOC significantly increased ($P<0.001$) the half-life ($T_{1/2}$; 19.90h), mean residence time (MRT; 26.86h) and area under the curve (AUC; 89.73% h/mL) of DOC in circulation, as compared DS ($T_{1/2}$; 4.79h, MRT; 5.96h, AUC; 24.24% h/ml,). These

results indicate that PolyDOC can circulate for a longer time in the blood circulation system than DS.

PolyDOC was found to be non-hemolytic (i.e., less than 5% hemoglobin released) at all concentrations examined (10μg/mL to 100μg/mL DOC equivalent concentration). However, more than 30% hemolytic activity was observed with DS formulation (100μg/mL). Main constitute in DS formulation is Tween 80, which had been reported to interact with cell membrane of RBC and cause significant hemolytic activity. Therefore PolyDOC are apparently more hemocompatible compared to DS formulation.

PolyDOC uptake in tissue was significant ($P<0.01$) in each organ than DS at 2mg/kg body weight dose equivalent to free DOC.

Results demonstrate that liver, lungs and spleen are the organs of preferential accumulation of ^{99m}Tc-PolyDOC. PolyDOC uptake was significantly high ($P<0.05$) in tumor compared to DS.

PolyDOC reduces significantly ($P<0.01$) the ratio between liver/blood than DS which indicates PolyDOC clearance was delayed compared to free DS formulation after IV injection of PolyDOC. Interestingly, PolyDOC showed high ratio of uptake between tumor and muscles and was significantly ($P <0.001$) higher than DS.

In conclusion, that block copolymers composed of a polypeptide segment and a polysaccharide moiety provide significant advantages in controlling both the vesicular structure and the biofunctionality. Such biomimetic self-assemblies combine high colloidal stability, biocompatibility and degradability, together with controlled release properties of anticancer drugs. The use of hyaluronan as the hydrophilic stabilizing block, combined to its specific ligand properties to CD44 glycoprotein receptors that are over-expressed in many cancers, provides a means to obtain synergy between structure and biofunctionality within a single material. Such an original approach opens new avenues in the preparation of multifunctional nano-devices or self targetable drug delivery system.